



HAL
open science

An interconnected discrete time cascaded semi-implicit differentiation

Loïc Michel, Malek Ghanes, Yannick Aoustin, Jean-Pierre Null Barbot

► **To cite this version:**

Loïc Michel, Malek Ghanes, Yannick Aoustin, Jean-Pierre Null Barbot. An interconnected discrete time cascaded semi-implicit differentiation. 2024. hal-04564290v2

HAL Id: hal-04564290

<https://hal.science/hal-04564290v2>

Preprint submitted on 11 May 2024

HAL is a multi-disciplinary open access archive for the deposit and dissemination of scientific research documents, whether they are published or not. The documents may come from teaching and research institutions in France or abroad, or from public or private research centers.

L'archive ouverte pluridisciplinaire **HAL**, est destinée au dépôt et à la diffusion de documents scientifiques de niveau recherche, publiés ou non, émanant des établissements d'enseignement et de recherche français ou étrangers, des laboratoires publics ou privés.

An interconnected discrete time cascaded semi-implicit differentiation

Loïc MICHEL, Malek GHANES, Yannick Aoustin and Jean-Pierre BARBOT

Abstract—This study is dedicated to the design of a digital differentiator for a triple integrator. A cascade of two interconnected semi-implicit Euler double differentiators approach is proposed. This allows the digital differentiator to benefit from similar structure of second order discrete-time homogeneous differentiators, such as modularity and more degree of freedom regarding the parameter settings. Numerical results are presented to support the rightness of the proposed method.

Index Terms—Discretization, Homogeneous differentiator, correcting terms, interconnected systems

I. INTRODUCTION

The use of a limited number of proprioceptive sensors helps reducing the costs of its implementation and increases its reliability (i.e. software sensor redundancy, expensive physical sensor, cost of maintenance, ...). Thus, the utilization of differentiators contributes to this effort to reduce the number of sensors on an experimental process while allowing its control. The digital implementation of differentiator algorithms is often necessary as a part of industrial and/or experimental processes that requires numerical estimation of derivative. Especially, discrete-time differentiators are relevant with respect to engineering applications: for example, the discrete-time optimal control based tracking differentiator [15] and the super-twisting algorithm [23] are two widely used algorithms but it is still a difficult problem to estimate the exact derivative signals from the noise-corrupted inputs [38].

Time discretization has a considerable influence on the behavior and properties of sliding mode multi-valued controls or differentiators [10]. In order to overcome some limitations of the classical sliding-mode, such as cancellation of the chattering effect as well as robustness of the estimation under lower sampling frequencies, Acary *et. al.* [2] introduce an implicit discretization technique. The principle of this method is to replace the classical sign function by an *implicit* projector and some recent successful experiments through implicit based sliding mode control algorithms have been obtained (see e.g. [17], [1], [18], [37], [7], [19], [8], [11] [21] and [9]). In the framework of the discrete homogeneous differentiation, the semi-implicit differentiator combines explicit terms with implicit ones including *projectors* in order to reduce the effects of chattering [28].

This work is supported by the ANR project DigitSlid ANR-18-CE40-0008-01.

L. MICHEL, M. GHANES and J.-P. BARBOT are with Nantes Université-École Centrale de Nantes-LS2N, UMR 6004 CNRS, Nantes, France {loic.michel, malek.ghanes}@ec-nantes.fr

Y. Aoustin is with Nantes Université-LS2N, UMR 6004 CNRS, Nantes yannick.aoustin@univ-nantes.fr

J.-P. BARBOT is also with QUARTZ EA 7393, ENSEA, Cergy-Pontoise, France barbot@ensea.fr

Inspired by the work of Andrieu *et al* [6], which proposes a continuous time cascade of interconnected second order differentiators, the authors presented recently the derivation of a cascaded version of second order semi-implicit homogeneous differentiator [26], [29]. Two stages of differentiators are considered for which the homogeneous degrees (exponent parameters) can be adjusted separately. In addition, in [27], the authors presented also a semi-implicit based third differentiator including additional Taylor expansion corrective terms (inspired from [5], [24]) to improve the precision.

The proposed contribution is to enhance the semi-implicit cascade version including corrections terms aiming to reduce the estimation error. Such implementation takes benefit from gain flexibility in order to tune the differentiators as well as modularity (i.e. by using the same structure of second order discrete-time differentiator on each part of the cascade).

The paper is outlined as follows. Section II recalls the background about the explicit and implicit Euler discretization. Section III is focused on the cascade of two discretized second order differentiators with correcting terms. Section IV, dedicated to simulations results, highlights the well founded of the proposed algorithms. The paper ends, in section V, with a conclusion and some perspectives.

II. EXPLICIT AND IMPLICIT DISCRETIZATION

Considering the following analytic autonomous system:

$$\dot{x} = f(x) \quad (1)$$

where $x \in \mathbb{R}^n$ is the state vector and $f(x)$ an analytic vector field. A formal solution in exponential Lie development [14], [32] is:

$$x(t + \delta) = e^{L_f \delta} \mathbf{I}_d|_{x(t)} = \sum_{i=0}^{\infty} \frac{\delta^i}{i!} L_f^i \mathbf{I}_d|_{x(t)} \quad (2)$$

with $L_f := \sum_{j=1}^n f_j \frac{\partial}{\partial x_j}$ the classical Lie derivative, $|_{x(t)}$ means that all functions are evaluated at $x(t)$ and $\frac{\delta^0}{0!} L_f^0 \mathbf{I}_d|_{x(t)} = x(t)$. For obvious computational reasons, the discretization is often truncated, which has also an advantage with respect to the zero dynamic under sampling [31], [39]. One of the ways of obtaining an exact solution to the discretization of equation (1) is for it to be nilpotent. Equation (1) is nilpotent [16], [20] if there exists an integer k such that:

$$e^{L_f \delta} \mathbf{I}_d|_{x(t)} = \sum_{i=0}^k \frac{\delta^i}{i!} L_f^i \mathbf{I}_d|_{x(t)} \quad (3)$$

Since the work of B. Brogliato and co-authors [3] on the discretization of differential inclusions dedicated to control

and/or observation under sampling, the question of implicit or explicit discretization has been raised, but what this meaning of both discretization types?

Equation (2) is the explicit discretization of (1), while the following equation is its implicit version:

$$x(t + \delta) = x(t) + \sum_{i=1}^{\infty} \frac{(-\delta)^i}{i!} \mathbf{L}_f^i \mathbf{I}_{d|x(t+\delta)} \quad (4)$$

This equation comes from a simple manipulation of the following equation:

$$x(t) = e^{\mathbf{L}_f(-\delta)} \mathbf{I}_{d|x(t+\delta)} = \sum_{i=0}^{\infty} \frac{(-\delta)^i}{i!} \mathbf{L}_f^i \mathbf{I}_{d|x(t+\delta)}$$

The advantages of Euler implicit discretization (i.e. approximation in $O(\delta^2)$) have been demonstrated in numerous articles for both control [22], [33] and differentiation [30], [34].

Let us recall the exact discretization for a double integrator, considering the following controlled and perturbed system:

$$\begin{aligned} \dot{x}_1 &= x_2 \\ \dot{x}_2 &= u + p \end{aligned} \quad (5)$$

where u is the control input and p a perturbation both are considered slowly variable with respect to the sampling period δ i.e. $\forall t > 0$ and $\forall \theta \in [0, \delta]$ $u(t+\theta) - u(t) \simeq 0$ and $p(t+\theta) - p(t) \simeq 0$. Then, for time periods of the order of δ , equation (5) can be rewritten as follows in term of triple integrator without input:

$$\begin{aligned} \dot{x}_1 &= x_2 \\ \dot{x}_2 &= x_3 + u \\ \dot{x}_3 &= 0 \end{aligned} \quad (6)$$

where $x_3 := p$.

From (4) and (3) the implicit discretization of (6) is:

$$\begin{aligned} x_1^+ &= x_1 + \delta x_2^+ - \frac{\delta^2}{2!} (x_3^+ + u^+) \\ x_2^+ &= x_2 + \delta (x_3^+ + u^+) \\ x_3^+ &= x_3 \end{aligned} \quad (7)$$

where $x_i, i \in \{1, 2, 3\}$, stands for $x_i(k\delta)$ and x_i^+ stands for $x_i((k+1)\delta)$.

III. CASCADE OF TWO SEMI-IMPLICIT DISCRETE DIFFERENTIATORS INCLUDING CORRECTION TERMS

In order to obtain more degrees of freedom in the parameter settings and to deal only with differentiators of order 2, this section presents a cascade of semi-implicit Euler order 2 differentiators with correcting terms.

This approach is inspired by the continuous-time articles [4] and [12]. In [4], a cascade of differentiators is introduced and in [12], a step-by-step observer is proposed. Nevertheless, the basic idea still remains to use the equivalent vector principle [36], which is only possible under sampling in implicit Euler discretization [6] and semi-implicit Euler discretization [25], [30], [34].

The cascade of two semi-implicit Euler double differentiators for system (7), is then proposed as follows and depicted in Fig 1:

(a) the first differentiator stage is:

$$\begin{aligned} z_1^+ &= z_1 + \delta(z_2^+ + \lambda_1 |e_1|^{\alpha_1} \mathcal{N}_1) - \frac{\delta^2}{2} (\bar{E}_2 \bar{z}_2^+ f_{wd} + u^+) \\ z_2^+ &= z_2 + \delta(\lambda_2 |e_1|^{2\alpha_1-1} \mathcal{N}_2 + \bar{E}_2 \bar{z}_2^+ f_{wd} + u^+) \end{aligned} \quad (8)$$

where $e_1 = x_1 - z_1$ (i.e. $e_1 = 0$ defines the sliding surface), including the notation $[\bullet]^{\alpha_1} = |\bullet|^{\alpha_1} \text{sgn}(\bullet)$. $\bar{z}_2^+ f_{wd}$ is the correction term that comes from the second differentiator. The associated projectors $\mathcal{N}_{(q,\theta)}$ with $q \in \{1, 2\}$, $\alpha \in [\frac{2}{3}, 1[$ and $\theta \in [0, 1[$ are defined by:

$$\mathcal{N}_{(q,\theta)} := \begin{cases} \text{if } (1-\theta)|e_1|^{q(1-\alpha)} < \lambda_q \delta^q \\ \quad \rightarrow \mathcal{N}_q = (1-\theta) \frac{[e_1]^{q(1-\alpha)}}{\lambda_q h^q} \\ \text{if } (1-\theta)|e_1|^{q(1-\alpha)} \geq \lambda_q \delta^q \\ \quad \rightarrow \mathcal{N}_q = \text{sgn}(e_1) \end{cases} \quad (9)$$

Moreover, E_2 is defined such as:

$$E_2 := \begin{cases} \text{if } (1-\theta)|e_1|^{2(1-\alpha)} < \lambda_2 \delta^2 & \rightarrow E_2 = 1 \\ \text{if } (1-\theta)|e_1|^{2(1-\alpha)} \geq \lambda_2 \delta^2 & \rightarrow E_2^+ = 0 \end{cases} \quad (10)$$

(b) by considering the general definition of (9) and (10), the second differentiator is:

$$\bar{z}_1^+ = \bar{z}_1 + \delta(\bar{z}_2^+ + u^+ + \bar{\lambda}_1 |\bar{e}_1|^{\alpha_2} \bar{\mathcal{N}}_1) \quad (11)$$

$$\bar{z}_2^+ = \bar{z}_2 + \delta \bar{\lambda}_2 |\bar{e}_1|^{2\alpha_2-1} \bar{\mathcal{N}}_2 \quad (12)$$

where $\bar{e}_1 = \bar{x}_1 - \bar{z}_1$ with $\bar{x}_1 = z_2$.

$$\bar{z}_2^+ f_{wd} = \bar{z}_2 f_{wd} + \lambda f_{wd} (\bar{z}_2 - \bar{z}_2 f_{wd}) \quad (13)$$

Remark that (13) has been designed using the z transform of first order low pass filter with $s = \frac{1-z^{-1}}{\delta}$. Concerning the tuning of the parameters, from the gained experience, the amplification parameters $\lambda_1, \lambda_2, \bar{\lambda}_1$, and $\bar{\lambda}_2$ are set to ensure the stability following a standard pole placement. The parameters α_1 and α_2 are chosen to make a trade-off between the noise and perturbation rejection (see [13] for the continuous case). Moreover, the role of the parameter θ is to reduce the sensitivity with respect to the noise inside the projector. Practically, these parameters can be set using a direct estimation with respect to the dynamics and the power of noise, or set using an optimization algorithm (using e.g. the BFO algorithm [35]).

Proposition 1: For $\theta = 0$, a sufficiently small $\delta > 0$, an appropriate choice of the parameters $\lambda_i, \bar{\lambda}_i$ for $i \in \{1, 2\}$ and λf_{wd} , the cascade of differentiators (8)-(11) converges asymptotically to the solution of (7).

Considering the observation error, after convergence ($e_1 \rightarrow 0$) the first row gives:

$$e_1^+ = \delta e_2^+ - \frac{\delta^2}{2} (x_3^+ - \bar{E}_2 \bar{z}_2^+ f_{wd}) \quad (14)$$

This equation (14) gives after one more iteration:

$$e_2 = \frac{e_1}{\delta} + \frac{\delta}{2} (x_3 - \bar{E}_2 \bar{z}_2 f_{wd}) \quad (15)$$

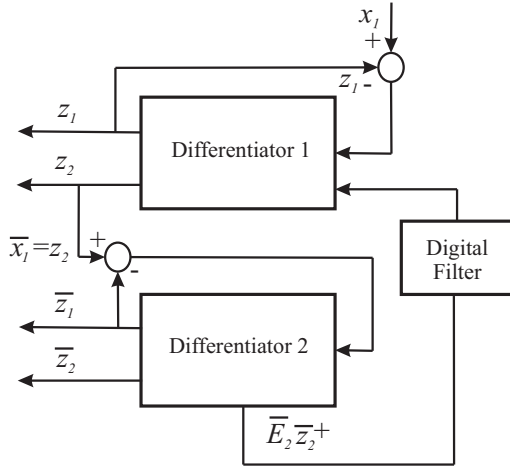


Fig. 1: Cascade of two differentiators under sampling with correction terms.

Using (15) in the second row of the observation error one obtains:

$$e_2^+ = \frac{e_1}{\delta} + \frac{\delta}{2}(x_3 - \bar{E}_2 \bar{z}_2 f_{wd}) + \delta(\lambda_2 |e_1|^{2\alpha_1 - 1} \bar{N}_2 + x_3^+ - \bar{E}_2 \bar{z}_2^+ f_{wd}) \quad (16)$$

After convergence (cancellation of $\frac{e_1}{\delta}$), one has:

$$e_2^+ = \frac{\delta}{2}(x_3 - \bar{E}_2 \bar{z}_2 f_{wd}) + \delta(x_3^+ - \bar{E}_2 \bar{z}_2^+ f_{wd}) \quad (17)$$

From the fact that the input of the second semi-implicit Euler double integrator is $y_2 = z_2 = x_2 - e_2$, and $\bar{x}_1 = z_2$ and $\bar{x}_2 = x_3$ are set. The predicted state calculated by the second differentiator is:

$$\begin{aligned} \bar{x}_1^+ &= \bar{x}_1 + e_2 + \delta x_3^+ - e_2^+ \\ \bar{x}_2^+ &= \bar{x}_2 \end{aligned} \quad (18)$$

From (11) and (18) the observation error for \bar{e}_1 is:

$$\bar{e}_1^+ = \bar{x}_1 + e_2 + \delta x_3^+ - e_2^+ - \bar{z}_1 - \delta(\bar{z}_2^+ + \bar{\lambda}_1 |\bar{e}_1|^{\alpha_2} \bar{N}_1)$$

after convergence (i.e. cancellation of $\bar{x}_1 - \bar{z}_1$ by $\delta \bar{\lambda}_1 |\bar{e}_1|^{\alpha_2} \bar{N}_1$), one obtains:

$$\bar{e}_1^+ = e_2 + \delta \bar{x}_2^+ - e_2^+ - \delta \bar{z}_2^+ \quad (19)$$

The second row of the second differentiator is:

$$\bar{z}_2^+ = \bar{z}_2 + \delta \bar{\lambda}_2 |\bar{e}_1|^{2\alpha_2 - 1} \bar{N}_2 \quad (20)$$

Moreover, as $\bar{x}_2 = x_3$, one has:

$$\bar{x}_2^+ = \bar{x}_2 \quad (21)$$

and the second state of observation error is: $\bar{e}_2 = \bar{x}_2 - \bar{z}_2 = x_3 - \bar{z}_2$.

Rewriting (19) such as:

$$\bar{e}_1 = e_2^- + \delta \bar{x}_2 - e_2 - \delta \bar{z}_2 \quad (22)$$

this implies that $\bar{e}_2 = \bar{x}_2 - \bar{z}_2$ is given by:

$$\bar{e}_2 = \frac{\bar{e}_1}{\delta} + \frac{e_2 - e_2^-}{\delta} \quad (23)$$

Using (23) in the second row of the observation error of the second differentiator leads to:

$$\bar{e}_2^+ = \frac{\bar{e}_1}{\delta} + \frac{e_2 - e_2^-}{\delta} - \delta \bar{\lambda}_2 |\bar{e}_1|^{2\alpha_2 - 1} \bar{N}_2 \quad (24)$$

after convergence (i.e. cancellation of $\frac{\bar{e}_1}{\delta}$), one has:

$$\bar{e}_2^+ = \frac{e_2 - e_2^-}{\delta} \quad (25)$$

Is it possible to know x_3^+ ? Yes, thanks to the available observation errors i.e e_1 and \bar{e}_1 . Considering firstly that both differentiators are in the sliding strip, then using two times equation (15) in (19) in order to substitute e_2 and e_2^+ , this gives:

$$\bar{e}_1^+ = \frac{e_1}{\delta} + \frac{\delta}{2}(x_3 - \bar{z}_2 f_{wd}) - \left(\frac{e_1^+}{\delta} + \frac{\delta}{2}(x_3^+ - \bar{z}_2^+ f_{wd})\right) + \delta(x_3^+ - \bar{z}_2^+) \quad (26)$$

which gives after a reordering:

$$\bar{e}_1^+ + \frac{e_1^+ - e_1}{\delta} = \frac{\delta}{2}(x_3 - \bar{z}_2 f_{wd}) - \frac{\delta}{2}(x_3^+ - \bar{z}_2^+ f_{wd}) + \delta(x_3^+ - \bar{z}_2^+)$$

The parameter λ_{fwd} is chosen such that in (13), $\bar{z}_2 f_{wd}$ converges asymptotically to \bar{z}_2 . Since $x_3^+ = x_3$, then asymptotically the following equation is verified:

$$\bar{e}_1^+ + \frac{e_1^+ - e_1}{\delta} = \delta(x_3^+ - \bar{z}_2^+)$$

which gives:

$$x_3^+ = x_3 = \frac{\bar{e}_1}{\delta} + \frac{e_1^+ - e_1}{\delta^2} + \bar{z}_2^+ \quad (27)$$

Finally, as x_3 is asymptotically estimated then asymptotically $e_1 = e_2 = \bar{e}_1 = \bar{e}_2 = 0$ and $\bar{x}_2 = \bar{z}_2 = x_3$. \square

Remark 1: In (13), if $\lambda_{fwd} = 1$ then $\bar{z}_2^+ f_{wd}$ is equal to \bar{z}_2^+ and due to the fact that the second differentiator is computed after the first one, then this introduces an extra delay in the correction terms $\bar{z}_2 f_{wd}$, which leads to instability. In the same way, the phenomena occurs if the second differentiator is computed before the first one. Viewed that the input of the second differentiator is the output of the the first one with one step of delay and introduce also one delay in the correction terms and instability, this is the reason of using (13).

IV. NUMERICAL RESULTS AND DISCUSSION

The implicit double integrator system (6) is simulated considering the following initial conditions: $x_1(0) = x_2(0) = x_3(0) = 0$ and the particular input u such as $u = 1$ if $t < 30$ s and $u = -1$ if $t \geq 30$ s is applied to the system. The perturbation p is set to $p = 0.5$.

The gains and parameters for each stage of the cascade are set as follows:

- (a) $\lambda_1 = 2 \cdot 10^2$, $\lambda_2 = 4 \cdot 10^4$ and $\alpha_1 = 0.95$;
- (b) $\bar{\lambda}_1 = 2 \cdot 10^2$, $\bar{\lambda}_2 = 4 \cdot 10^4$ and $\alpha_2 = 0.98$.

All simulations are running over 60 sec (and the input u switches between $+1$ and -1 at $t = 30$ sec). The following results present five cases illustrating different configurations

of the differentiator¹. For all cases, the initial conditions of the cascade is set to $z_1(0) = -0.7$, $z_2(0) = -1$, $\bar{z}_1(0) = 0.5$, $\bar{z}_2(0) = 1$. The θ projector is in action only in the case 5 (set to $\theta = 0.5$) and is set to $\theta = 0$ in the other cases.

The parameter $\lambda_{fwd} = 0.3$ has been set to give a slow interconnection response (the influence of λ_{fwd} will be discussed later).

- *Case 1 : Cascade with the correction terms and the knowledge of u*
 Figures 2 and 3 depict respectively the states estimation and the estimation error considering the inclusion of the correction terms and knowledge of u .

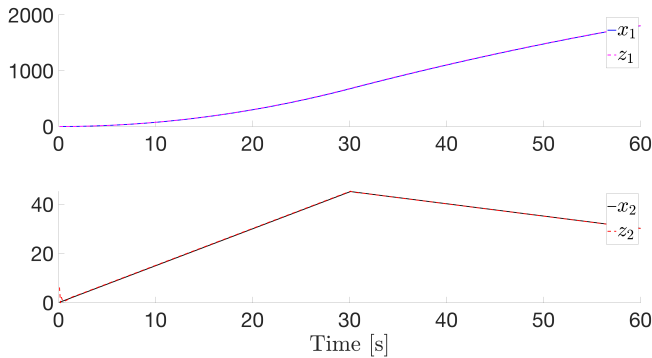


Fig. 2: State estimation (with correction terms and knowledge of u).

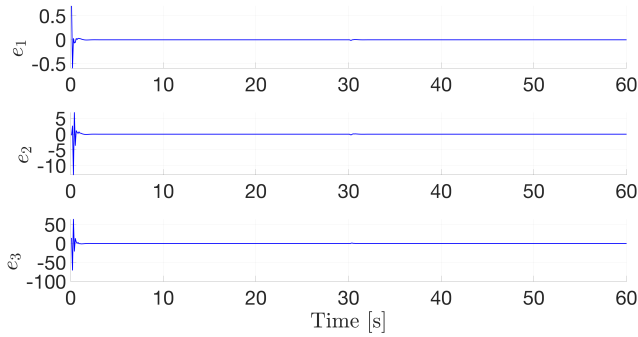


Fig. 3: Differentiation estimated errors (with correction terms and knowledge of u).

- *Case 2 : Cascade with the correction terms and without the knowledge of u*
 Figure 4 depicts the estimation error considering the inclusion of the correction terms but without the knowledge of u .
- *Case 3 : Cascade without the correction terms and without the knowledge of u*
 Figure 5 depicts the estimation error without the correction term and without the knowledge of u .

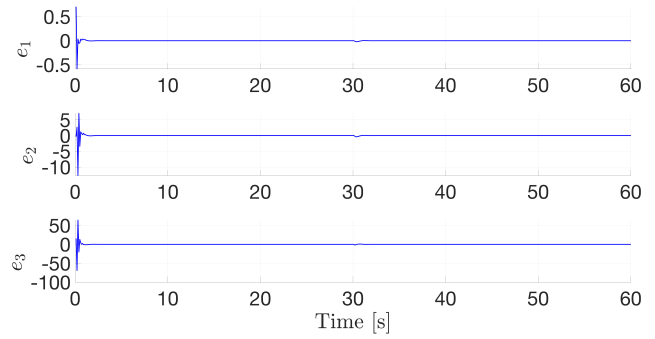


Fig. 4: Differentiation estimated errors (with correction terms and without knowledge of u).

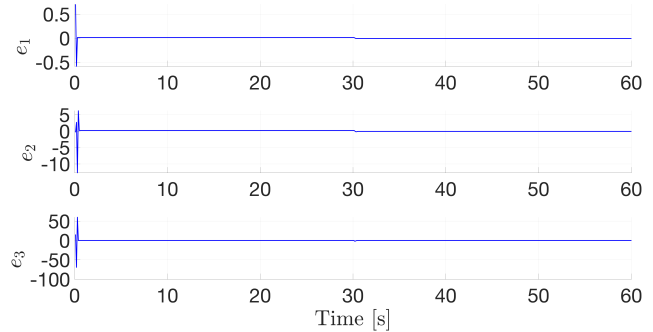


Fig. 5: Differentiation estimated errors (without correction terms and without knowledge of u).

- *Case 4 : Cascade with the correction terms and the knowledge of u and the presence of noise for $\theta = 0$*
 Figures 6 and 7 depict respectively the states estimation and the estimation error, for which the noise² is obtained by a random generator that is multiplied by $\eta_0 = 0.1$. This noise is added to the x_1 state.

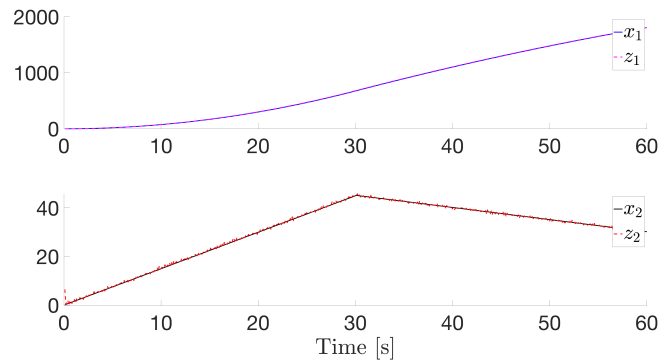


Fig. 6: State estimation (with correction terms and knowledge of u) for $\theta = 0$.

- *Case 5: Cascade with the correction terms and the knowledge of u and the presence of noise for $\theta > 0$*

¹Simulation code can be found in the repository:
<https://github.com/LoicMichelControl/Interconnected-Cascaded-Semi-Implicit-Differentiation---Supplementary-Material.git>.

²The noise is computed under Matlab® using the instruction `eta0 * rand()` where `eta0` is a factor that multiplies the noise.

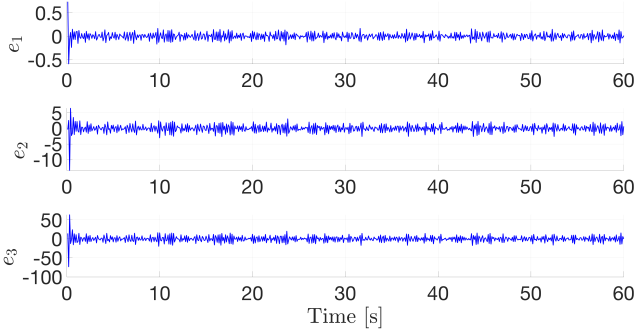


Fig. 7: Differentiation estimated errors (including correction terms and knowledge of u) in presence of noise for $\theta = 0$.

Figure 8 depicts respectively the states estimation and the estimation error, for which a noise of amplitude $\eta_0 = 0.1$ is added to the x_1 state. In this case, the efficiency of the θ parameter (included in the projector (9)) is evaluated considering $\theta = 0.5$.

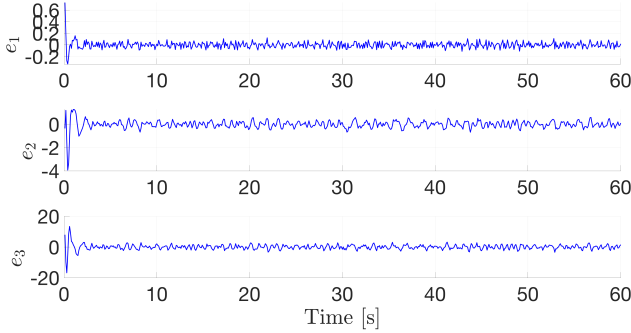


Fig. 8: Differentiation estimated errors (without correction terms and knowledge of u) for $\theta = 0.5$.

The Tables I and II summarizes the properties of the errors with respect to each studied case: the averaged errors, denoted respectively e_1^a , e_2^a , and e_3^a , as well as the sum of square errors (SSE), denoted respectively e_1^s , e_2^s , and e_3^s are calculated over the last 15 sec. The maximum of the errors over the 60 sec is denoted respectively e_1^m , e_2^m , and e_3^m .

case #	e_1^a	e_1^m	e_2^a	e_2^m	e_3^a	e_3^m
1	$< 10^{-10}$	0.70	$< 10^{-10}$	12.8	$< 10^{-10}$	70.2
2	$< 10^{-10}$	0.70	$< 10^{-10}$	12.6	$< 10^{-10}$	69.2
3	-0.004	0.7	-0.07	12.69	$< 10^{-10}$	69.2
4	0.0004	0.78	-0.008	14.4	0.04	78
5	0.0002	0.75	0.005	3.82	0.017	15.9

TABLE I: Properties of the differentiation error (averaged error and max. of the error) with respect to each case.

The cases 1 and 2 show a great precision thanks to the correction terms, and the knowledge of the input u is slightly better to estimate properly the perturbation p . However, when the correction terms are not in effect, like in the case 3, the precision is largely decreased on e_1 and e_2 , highlighting the accuracy of the forwarded information from the highest

case #	e_1^s	e_2^s	e_3^s
1	$< 10^{-10}$	$< 10^{-10}$	$< 10^{-10}$
2	$< 10^{-10}$	$< 10^{-10}$	$< 10^{-10}$
3	$< 10^{-10}$	$< 10^{-10}$	$< 10^{-10}$
4	0.0049	1.32	57.8
5	0.0016	0.041	1.21

TABLE II: Properties of the differentiation error (sum of square error) with respect to each case.

derivative stage of the differentiator to "refine" the Taylor expansion on the first stage, giving hence more accuracy to the estimation. Let us emphasize the fact that the high values of the λ parameters that have been chosen for this particular system, allow a good initial transient toward the "tracking" of the estimation. In addition, the intrinsic tuning flexibility of the cascade allows giving different α parameters, thus allowing a slightly better rejection of the noise in the second differentiation stage by choosing $\alpha_2 > \alpha_1$. However, dealing with two separate stages may introduce oscillations due to the interconnection (for which the lower stage has to "absorb" stiff changes of the perturbation estimation), which can be overcome using a simple first order filter (whose time-constant has to be chosen to damp transient of the forwarded high order derivative estimation). Remark that setting $\lambda_{fwd} = 1$ induces strong oscillations on the estimation due to the delay in the correction terms that may create instability. At the opposite, a small λ_{fwd} slows down the transient of the interconnection inducing therefore a very slow global dynamics of the cascade. A proper choice of λ_{fwd} is a compromise between the time response of the estimation and the whole stability. From the noise rejection point of view, the previous experience has shown that the use of θ projector has improved greatly (about fifty time) the accuracy of the rejection as shown by the SSE index between the case 4 ($\theta = 0$) and the case 5 ($\theta = 0.5$) in the Table II. Another advantage of $\theta > 0$ is the attenuation of e_2^m and e_3^m for which the overshoots are attenuated in amplitude but stay longer in time. Combined with the proposed interconnected architecture of differentiation, it improves slightly the reduction of the noise as shown in the case 5 (for which θ has been set to 0.5), compared with the case 4 ($\theta = 0$) since the cascade offers already good filtering properties.

Such properties of filtering associated to the interconnection offer kind of modularity of the proposed architecture, hence using a "bloc" of differentiation including the flexibility of tuning separately the parameters as well as taking from the benefit of the interconnections to improve the state estimation.

V. CONCLUSION

This work presented an interconnected cascade differentiator based on semi-implicit discrete differentiation. The proposed contribution aims to include correction terms in order to improve the accuracy. Numerical simulations highlight the well founded of the proposed approach. Future perspectives include to develop an optimization procedure to better tune

the parameters and also use the variable exponent in order to adapt the degree of homogeneity with respect to the noise.

ACKNOWLEDGMENTS

This work was supported partially by the ANR project DigitSlid ANR-18-CE40-0008-01 (<https://anr.fr/Project-ANR-18-CE40-0008>) and by the GOWIBA project that is funded by the Carnot Institute Marine Engineering Research for Sustainable, Safe and Smart Seas. Jean-Pierre Barbot is supported with (*Région Pays de la Loire*) Connect Talent GENYDROGENE project.

REFERENCES

- [1] V. Acary, B. Brogliato, and Y. Orlov. Chattering-free digital sliding-mode control with state observer and disturbance rejection. *IEEE Trans. on Automatic Control*, 57(5):1087–1101, 2012.
- [2] Vincent Acary and Bernard Brogliato. Implicit Euler numerical scheme and chattering-free implementation of sliding mode systems. *Systems & Control Letters*, 59(5):284 – 293, 2010.
- [3] Vincent Acary and Bernard Brogliato. Implicit euler numerical scheme and chattering-free implementation of sliding mode systems. *Systems Control Letters*, 59(5):284–293, 2010.
- [4] Vincent Andrieu, Laurent Praly, and Alessandro Astolfi. Homogeneous approximation, recursive observer design, and output feedback. *SIAM J. on Control and Optimization*, 47(4):1814–1850, 2008.
- [5] Jean-Pierre Barbot, Arie Levant, Miki Livne, and Davin Lunz. Discrete differentiators based on sliding modes. *Automatica*, 112:108633, 2020.
- [6] Pauline Bernard, Laurent Praly, Vincent Andrieu, and Hassan Hammouri. On the triangular canonical form for uniformly observable controlled systems. *Automatica*, 85:293–300, 2017.
- [7] B. Brogliato and A. Polyakov. Globally stable implicit Euler time-discretization of a nonlinear single-input sliding-mode control system. In *2015 54th IEEE Conf. on Decision and Control*, pages 5426–5431, 2015.
- [8] B. Brogliato, A. Polyakov, and D. Efimov. The implicit discretization of the super-twisting sliding-mode control algorithm. In *2018 15th Int. Workshop on Variable Structure Systems (VSS)*, pages 349–353, 2018.
- [9] B. Brogliato, A. Polyakov, and D. Efimov. The implicit discretization of the super-twisting sliding-mode control algorithm. *IEEE Trans. on Automatic Control*, pages 1–1, 2019.
- [10] Bernard Brogliato and Andrey Polyakov. Digital implementation of sliding-mode control via the implicit method: A tutorial. *International Journal of Robust and Nonlinear Control*, 31(9):3528–3586, 2021.
- [11] Jose Eduardo Carvajal-Rubio, Juan Diego Sánchez-Torres, Michael Defoort, Mohamed Djemai, and Alexander G. Loukianov. Implicit and explicit discrete-time realizations of homogeneous differentiators. *International Journal of Robust and Nonlinear Control*, 31(9):3606–3630, 2021.
- [12] T. Floquet and J. P. Barbot. Super twisting algorithm-based step-by-step sliding mode observers for nonlinear systems with unknown inputs. *International Journal of Systems Science*, 38(10):803–815, 2007.
- [13] M. Ghanes, J. P. Barbot, L. Fridman, A. Levant, and R. Boisliveau. A new varying-gain-exponent-based differentiator/observer: An efficient balance between linear and sliding-mode algorithms. *IEEE Trans. on Automatic Control*, 65(12):5407–5414, 2020.
- [14] W Gröbner. Die lie-reihen und ihre anwendungen, springer verlag, berlin (1960)(it. transi.: 1973, le serie di lie e le loro applicazioni). 1973.
- [15] J. Han. From pid to active disturbance rejection control. [*IEEE Transactions on Industrial Electronics*, 56(3):900–906, 2009.
- [16] Henry Hermes. Nilpotent approximations of control systems and distributions. *SIAM Journal on Control and Optimization*, 24(4):731–736, 1986.
- [17] O. Huber, V. Acary, and B. Brogliato. Comparison between explicit and implicit discrete-time implementations of sliding-mode controllers. In *52nd IEEE Conf. on Decision and Control*, pages 2870–2875, 2013.
- [18] O. Huber, V. Acary, and B. Brogliato. Enhanced matching perturbation attenuation with discrete-time implementations of sliding-mode controllers. In *2014 European Control Conference*, pages 2606–2611, 2014.
- [19] O. Huber, V. Acary, and B. Brogliato. Lyapunov stability and performance analysis of the implicit discrete sliding mode control. *IEEE Trans. on Automatic Control*, 61(10):3016–3030, 2016.
- [20] Matthias Kawski. Nilpotent lie algebras of vectorfields. *Journal für die Reine und Angewandte Mathematik*, 1988(388):1–17, 1988. Funding Information: *) This work was supported by NSF Grant DMS 8500911 and is part of the doctoral dissertation of the author at the University of Colorado, Boulder.
- [21] Stefan Koch and Markus Reichhartinger. Discrete-time equivalent homogeneous differentiators. In *2018 15th International Workshop on Variable Structure Systems (VSS)*, pages 354–359, 2018.
- [22] A. Levant. Sliding order and sliding accuracy in sliding mode control. *Int. J. of Control*, 58(6):1247–1263, 1993.
- [23] Arie Levant. Robust exact differentiation via sliding mode technique. *automatica*, 34(3):379–384, 1998.
- [24] Miki Livne and Arie Levant. Proper discretization of homogeneous differentiators. *Automatica*, 50(8):2007–2014, 2014.
- [25] L. Michel, M. Ghanes, F. Plestan, Y. Aoustin, and J.P. Barbot. Semi-implicit Euler discretization for homogeneous observer-based control: one dimensional case. In *Proc. of the IFAC-V 2020, World Congress*, Berlin, Germany, July 2020.
- [26] L. Michel, S. Selvarajan, M. Ghanes, F. Plestan, Y. Aoustin, and J. P. Barbot. An experimental investigation of discretized homogeneous differentiators: pneumatic actuator case. *IEEE Journal of Emerging and Selected Topics in Industrial Electronics*, 2(3):227–236, 2021.
- [27] Loïc Michel, Malek Ghanes, Yannick Aoustin, and Jean-Pierre Barbot. A Third order Semi-Implicit Homogeneous differentiator: Experimental Results. In *International Workshop on Variable Structure Systems and Sliding Mode Control*, Rio de Janeiro, Brazil, September 2022.
- [28] Loïc Michel, Malek Ghanes, Franck Plestan, Yannick Aoustin, and Jean-Pierre Barbot. Semi-implicit euler discretization for homogeneous observer-based control: one dimensional case. *IFAC-PapersOnLine*, 53(2):5135–5140, 2020. 21st IFAC World Congress.
- [29] Loïc Michel, Malek Ghanes, Franck Plestan, Yannick Aoustin, and Jean-Pierre Barbot. Semi-implicit homogeneous euler differentiator for a second-order system: Validation on real data. In *2021 60th IEEE Conference on Decision and Control (CDC)*, pages 5911–5917, 2021.
- [30] Mohammad Rasool Mojallzadeh, Bernard Brogliato, Andrey Polyakov, Subiksha Selvarajan, Loïc Michel, Franck Plestan, Malek Ghanes, Jean-Pierre Barbot, and Yannick Aoustin. Discrete-time differentiators in closed-loop control systems: experiments on electro-pneumatic system and rotary inverted pendulum. *HAL-INRIA [Research Report hal-031225960]*, 2021.
- [31] S. Monaco and D. Normand-Cyrot. Zero dynamics of sampled nonlinear systems. *Systems & Control Letters*, 11(3):229–234, 1988.
- [32] S. Monaco and D. Normand-Cyrot. Issues on nonlinear digital control. *European Journal of Control*, 7(2):160–177, 2001.
- [33] Wilfrid Perruquetti, Thierry Floquet, and Emmanuel Moulay. Finite-time observers: application to secure communication. *IEEE Trans. on Automatic Control*, 53(1):356–360, 2008.
- [34] Andrey Polyakov. *Analysis of Homogeneous Dynamical Systems*, pages 225–270. Springer International Publishing, Cham, 2020.
- [35] Margherita Porcelli and Philippe L. Toint. Bfo, a trainable derivative-free brute force optimizer for nonlinear bound-constrained optimization and equilibrium computations with continuous and discrete variables. *ACM Trans. Math. Softw.*, 44(1), June 2017.
- [36] Vadim Utkin. *Sliding Modes and their Applications in Variable Structure Systems*. MIR publishers (Original version in Russian (1974)), Moscow, 1978.
- [37] B. Wang, B. Brogliato, V. Acary, A. Boubakir, and F. Plestan. Experimental comparisons between implicit and explicit implementations of discrete-time sliding mode controllers: Toward input and output chattering suppression. *IEEE Trans. on Control Systems Technology*, 23(5):2071–2075, 2015.
- [38] Juan Wang, Hehong Zhang, Gaoxi Xiao, Zhihong Dan, Song Zhang, and Yunde Xie. A comparison study of tracking differentiator and robust exact differentiator. In *2020 Chinese Automation Congress (CAC)*, pages 1359–1364, 2020.
- [39] K.J. Åström, P. Hagander, and J. Sternby. Zeros of sampled systems. *Automatica*, 20(1):31–38, 1984.